# X-RAY SPECTRAL STUDIES OF THE ELECTRONIC STRUCTURE OF URANYL FLUORITE UO$_2$F$_2$

by

**Igor O. UTKIN[1], Yury A. TETERIN[1], Vladimir A. TEREHOV[2], Mikhail V. RYZHKOV[3], Anton Yu. TETERIN[1], and Labud VUKCHEVICH[4]**

This work interpreted the fine X-ray photoelectron spectral structure of the low binding energy electrons (0-40 eV) and X-ray O$_{4,5}$(U) emission spectral structure from UO$_2$F$_2$ taking into account the relativistic X$_\alpha$ discrete variation (RX$_\alpha$-DV) calculation for the [(UO$_2$)F$_6$]$^{4-}$(D$_{6h}$) cluster reflecting an uranium close environment in UO$_2$F$_2$. The U5f electrons were shown to participate directly in the chemical bond formation. The U6p electrons were shown to participate not only in formation of the inner valence molecular orbitals, but also in formation of the outer valence molecular orbitals. The inner valence molecular orbitals sequence order in the binding energy range 12-40 eV was established. It is important for development of the technique of interatomic distance determination in the axial direction and equatorial plane of uranyl compounds on the X-ray photoelectron spectral basis.

*Key words: X-ray photoelectron spectroscopy, outer and inner valence molecular orbitals*

## INTRODUCTION

The low binding energy (0-50 eV) X-ray photoelectron spectroscopy (XPS) from uranyl fluorite (UO$_2$F$_2$) exhibits a complex fine structure attributed to the outer valence molecular orbitals (OVMO) and inner valence molecular orbitals (IVMO) electrons [1-3]. This spectrum reflects the band structure and is observed as several [eV] wide bands. In UO$_2$F$_2$ these IVMOs are built from the U6p and O(F)2s shells. A strong U6p-O(F)2s atomic orbital (AO) overlap for the [(UO$_2$)F$_6$]$^{6-}$(D$_{6h}$) cluster in the non-relativistic approximation was theoretically shown in [4, 5] and for the first time experimentally confirmed on the basis of the outer-core shells binding energy differ-

Authors' addresses:
[1] Russian Research Center "Kurchatov Institute"
1, Kurchatov square, Moscow 123182, Russia
[2] Voronezh State University, Voronezh, Russia
[3] Institute of Solid-State Chemistry of Ural Dept. of RAS,
Ekaterinburg, Russia
[4] Faculty of Natural Sciences and Mathematics,
University of Montenegro
P. O. Box 211, 81000 Podgorica, Serbia and Montenegro

E-mail addsess of corresponding author:
utkin@ignph.kiae.ru (I. O. Utkin)

ences for uranyl fluorite in [1, 6]. It allowed a qualitative identification of the high resolution X-ray O$_{4,5}$(U) emission spectral structure from UO$_2$F$_2$ [4, 7], which appeared to be an extra experimental corroboration for the IVMO formation in UO$_2$F$_2$.

According to earlier suggestions, the An5f- electrons are supposed to get promoted to, for example, the An6d atomic orbitals before the chemical bond formation. However, the theoretical calculations show that the An5f atomic shells can participate directly in the formation of molecular orbitals (MO) in actinide compounds [1]. This principally novel fact needs an experimental confirmation so in this work we measured high resolution X-ray O$_{4,5}$(U) emission spectral structures. However, in the absence of relativistic calculations of the UO$_2$F$_2$ electronic structure a correct interpretation of the XPS can not be achieved. In this work we interpreted the fine low binding energy XPS and X-ray emission spectral (XES) structures from UO$_2$F$_2$ taking into account the relativistic X$_\alpha$ discrete variation method (RX$_\alpha$-DVM) calculation of the electronic structure for the [(UO$_2$)F$_6$]$^{4-}$(D$_{6h}$) cluster reflecting an uranium close environment in UO$_2$F$_2$.

## EXPERIMENTAL

The XPS method is based on the photoeffect phenomenon in which XPS spectrum shows a dependence

of the number of photoelectrons on the binding energy. XPS spectra of $UO_2F_2$ were measured with an electrostatic spectrometer HP 5950A Hewlett-Packard using monochromatic $AlK_{\alpha 1,2}$ ($hv = 1486.6$ eV) radiation in a vacuum of 1.3 10$^{-7}$ Pa at room temperature. The device resolution measured as full width on the half-maximum (FWHM) of the $Au4f_{7/2}$ line on the standard rectangular golden plate was 0.8 eV. The binding energies $E_b$ [eV] were measured relative to the binding energy of the C1s electrons from hydrocarbons absorbed on the sample surface accepted to be equal to 285.0 eV. The FWHM were measured relative to the width of the C1s line of hydrocarbons accepted to be equal to 1.3 eV. The error in determination of electron binding energies and the line widths did not exceed 0.1 eV and that of the relative line intensities was less than 10%.

$UO_2F_2$ sample was prepared from the fine-dispersed powder ground in the agate mortar as a thick dense layer with a flat surface pressed in indium on the metallic substrate. Elastic scattering related background in the XPS was subtracted as described by Shirley [8].

X-ray $O_{4,5}(U)$ emission spectra (XES) of $UO_2F_2$ reflecting the U6p and U5f states in the valence band were measured by a primary method with a spectrometer RSM-500 with an energy resolution of 0.3 eV. The spectra were recorded during 60 minutes [4]. The change of energy of incident electrons allowed varying an effective depth of analysis from 15 up to 50 nm. The area of an exited electronic beam was 5  5 mm$^2$. The samples were ground in the agate mortar and then as a powder were pressed in a silver plate, which was fastened on the anode of the X-ray tube with the special clamps. For the spectra registration the secondary electronic multiplier of an open type was used. As the photocathode a CsI film was applied. The spectra were recorded three times to avoid the influence of the sample composition changes. For calibration of energy position of spectrum peculiarities Zr (75.55 eV) and Nb (85.85 eV) lines were taken in the second order of reflection M .

The $[(UO_2)F_6]^{6-}(D_{6h})$ cluster [9] reflecting uranium close environment in $UO_2F_2$ is a $UO_2^{2+}$ ion surrounded in the equatorial plane by the six flourines (ligands). The interatomic distances used in the calculations were $R_{U-O} = 1.74$ 10$^{-10}$ m and $R_{U-L(F)} = 2.43$ 10$^{-10}$ m. The calculations for this cluster were done in relativistic $X_\alpha$ Discrete Variation (RX$_\alpha$-DV) approximation [10] based on the Dirac-Slater equation for the 4 component spinors being a linear combination of atomic orbitals from the solution of the relativistic task for the isolated atoms. The extended basis of numerical atomic orbitals from the solution of Dirac-Slater equation for the isolated atoms beside the filled included the vacant U7p states. The direct AO decomposition basis were symmetrized linear AO combinations converting by the irreducible representations of the binary groups $D_{6h}$. The numerical integration during the calculation of secular equation matrix elements was done by the number

of 4500 points spread in the cluster space. It provided the convergence of MO energies of not worse than 0.1 eV. The local exchange-correlation potential was taken as $X_\alpha$ with $\alpha$ equal to the mean atomic values. Since the clusters were the fragments of the crystal, the ligand AO population renormalization during the self-consisting was done. It allowed an effective account of the stoichiometry and charge redistribution between the ligands and surrounding crystal [10]. For the correct evaluation of the relativistic effects in $UO_2F_2$ the non-relativistic $X_\alpha$-DV calculations (NRX$_\alpha$-DV) for the same crystalline parameters were done [4, 10].

## RESULTS AND DISCUSSION

The low binding energy (0-40 eV) XPS from $UO_2F_2$ can be conditionally subdivided into the two ranges (fig. 1). The first one 0-12 eV shows the structure attributed to the OVMOs built mostly from the incompletely filled outer U5f,6d,7s and
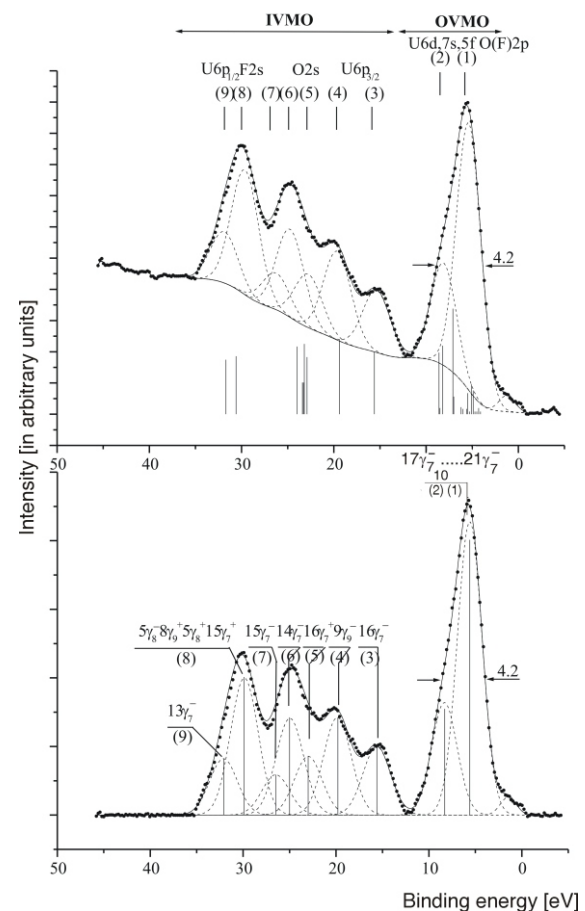


Figure 1. XPS from $UO_2F_2$ (a). The corresponding theoretical spectrum is given bellow as vertical bars. The same spectrum with subtracted background (b). Vertical bars show the spectrum on the basis of the theoretical and experimental data (see tab. 2). The dashed line shows the shape of the subtracted background (a) and subdivision into the separate components. Spectral intensity is in arbitrary units normalized by 100%

**Table 1. Relativistic X$_\alpha$-DV calculation results of the electronic structure for the UO$_2$F$_6^{4-}$(D$_{6h}$) cluster reflecting uranium close environment in UO$_2$F$_2$ at $R_{U\text{-}O}$ = 1.74 10$^{-10}$ m and $R_{U\text{-}L}$ = 2.43 10$^{-10}$ m**

MO composition (total electronic density per AO given in second header row)

| | MO | $-E$ [eV] | 6s | 6p$_{1/2}$ | 6p$_{3/2}$ | 6d$_{3/2}$ | 6d$_{5/2}$ | 7s | 5f$_{5/2}$ | 5f$_{7/2}$ | 7p$_{1/2}$ | 7p$_{3/2}$ | O2s | O2p | F2s | F2p |
|---|---|---|---|---|---|---|---|---|---|---|---|---|---|---|---|---|
| | | | $i$[a] 1.14 | 0.89 | 1.29 | 0.61 | 0.55 | 0.12 | 3.67 | 3.48 | 0.07 | 0.10 | 0.96 | 0.07 | 1.44 | 0.13 |
| OVMO | 24 $7^+$ | −13.0 | | | | 0.33 | 0.52 | 0.14 | | | | | | | | |
| | 25 $7^-$ | −6.0 | | | | 0.56 | 0.39 | 0.04 | | | | | | | | |
| | 14 $9^+$ | −5.7 | | | | | | | | | | 1.00 | | | | |
| | 22 $7^+$ | −5.7 | | | | | 1.00 | | | | | | | | | |
| | 24 $7^-$ | −5.3 | | | | | | 1.00 | | | | | | | | |
| | 23 $7^-$ | −4.5 | | | 0.33 | | | | 0.16 | 0.43 | | | | 0.08 | | |
| | 16 $9^-$ | −3.9 | | | | | | | | | 1.00 | | | | | |
| | 13 $9^+$ | −2.9 | | | | 0.77 | 0.18 | | | | | | | | | 0.05 |
| | 9 $8^+$ | −1.0 | | | | | 0.96 | | | | | | | | | 0.04 |
| | 15 $9^-$ | −0.9 | | | | | | | 0.10 | 0.72 | | 0.05 | | 0.13 | | |
| | 22 $7^-$ | 0.1 | | | | | | | 0.54 | 0.30 | | | | 0.15 | | |
| | 11 $8^-$ | 0.3 | | | | | | | 0.04 | 0.94 | | | | | | 0.02 |
| | 10 $8^-$ | 1.1 | | | | | | | | 0.98 | | | | | | 0.02 |
| | 9 $8^-$ | 1.4 | | | | | | | 0.91 | 0.05 | | | | | | 0.04 |
| | 14 $9^-$ | 2.1 | | | | | | | 0.80 | 0.14 | | | | 0.01 | | 0.05 |
| | $I_i$[a] | | | | 0.33 | 1.66 | 3.05 | 1.18 | 2.55 | 3.56 | 1.00 | 2.05 | | 0.37 | | 0.22 |
| | 21 $7^+$ [b] | 2.9 | | | | | | | | | | | | | | 1.00 |
| | 13 $9^-$ | 3.1 | | | 0.04 | | | | | | | | | 0.01 | | 0.95 |
| | 21 $7^-$ | 3.3 | | | | | | | | | | | | | | 1.00 |
| | 8 $8^+$ | 3.5 | | | | | | | | 0.03 | | | | | | 1.00 |
| | 8 $8^-$ | 3.7 | | | | | | | | 0.05 | | | | | | 0.97 |
| | 12 $9^-$ | 3.7 | | | | | | | | 0.06 | | | | | | 0.95 |
| | 20 $7^-$ | 3.9 | | | 0.08 | | | | | | | | | 0.04 | | 0.81 |
| | 7 $8^+$ | 3.9 | | | | | | | | | | | | | | 1.00 |
| | 12 $9^+$ | 3.9 | | | | | | | | | | | | 0.04 | | 0.96 |
| | 20 $7^+$ | 3.9 | | | | | | | | | | | | 0.08 | | 0.92 |
| | 11 $9^+$ | 4.1 | | | | | | | | | | | | | | 1.00 |
| | 11 $9^-$ | 4.3 | | | | | | | | 0.07 | | | | | | 1.00 |
| | 7 $8^-$ | 4.3 | | | | | | | | | | | | | | 0.93 |
| | 19 $7^-$ | 4.4 | | 0.01 | | | | | | | | | | | | 0.97 |
| | 19 $7^+$ | 4.8 | 0.03 | | | | | 0.02 | 0.01 | | | | | 0.03 | | 0.91 |
| | 6 $8^-$ | 5.0 | | | | | | | | | | | | | | 0.98 |
| | 6 $8^+$ | 5.8 | | | | | 0.18 | | 0.02 | | | | | | | 0.82 |
| | 10 $9^+$ | 5.8 | | | | | 0.19 | | | 0.26 | | | | | | 0.81 |
| | 18 $7^-$ | 5.9 | | | 0.17 | | | | | | | | | 0.26 | | 0.19 |
| | 18 $7^+$ | 7.0 | 0.07 | | | 0.02 | 0.04 | | 0.12 | 0.13 | | | 0.05 | 0.78 | | 0.04 |
| | 10 $9^-$ | 7.0 | | | 0.06 | | | | | | | | | 0.71 | | 0.02 |
| | 9 $9^+$ | 7.3 | | | | | 0.07 | | 0.07 | 0.03 | | | | 0.90 | | 0.03 |
| | 17 $7^-$ | 7.4 | | 0.03 | | | | | | | | | | 0.75 | | 0.01 |
| | 17 $7^+$ | 7.4 | | | | | 0.07 | | 0.18 | | | | | 0.87 | | 0.06 |
| | $\Sigma I_i$[a] | | 0.10 | 0.04 | 0.35 | 0.02 | 0.55 | 0.02 | 0.40 | 0.63 | | | 0.05 | 4.47 | | 17.3 |
| IVMO | 16 $7^-$ | 14.4 | | | 0.03 | | 0.47 | | | | | | 0.30 | 0.20 | | |
| | 9 $9^-$ | 18.2 | | | 0.87 | | | | | | | | | 0.05 | 0.06 | 0.01 |
| | 16 $7^+$ | 21.7 | 0.10 | | | 0.01 | 0.01 | | | | | | 0.85 | | 0.03 | |
| | 15 $7^-$ | 22.0 | | 0.12 | 0.04 | | | | | | | | 0.07 | | 0.76 | |
| | 5 $8^-$ | 22.0 | | | | | | | | | | | | | 1.00 | |
| | 8 $9^+$ | 22.1 | | | | | | | | | | | | | 1.00 | |
| | 5 $8^+$ | 22.2 | | | | | | | | | | | | | 1.00 | |
| | 15 $7^+$ | 22.8 | | | | | | | | | | | 0.03 | | 0.96 | |
| | 8 $9^-$ | 22.8 | | | 0.07 | | | | | | | | | | 0.93 | |
| | 14 $7^-$ | 24.4 | | 0.26 | 0.24 | | | | | | | | 0.24 | 0.04 | 0.22 | |
| | 13 $7^-$ | 30.5 | | 0.56 | 0.04 | | | | | | | | 0.29 | 0.10 | 0.01 | |
| | 14 $7^+$ | 46.4 | 0.80 | | | | | | | | | | 0.15 | 0.04 | | |
| | $\Sigma I_i$[a] | | 1.00 | 0.97 | 1.73 | 0.01 | 0.01 | | | | | | 1.93 | 0.44 | 5.97 | 0.01 |

[a] Total electronic densities per one electron
[b] Upper filled molecular orbital

O(F)2p AOs (tab. 1). The second one 12-40 eV shows the IVMO related fine structure. These IVMOs are built mostly from the completely filled inner valence U6p and O(F)2s AOs. The fact that the IVMO XPS parameters correlate with uranium close environment structure in compounds encouraged this subdivision [11]. The OVMO XPS structure has three typical features and can be subdivided into the three components. Since the low binding energy component at $E_b$ 1.5 eV is apparently due to the admixture of the U$^{4+}$ ions, it will not be considered here. The IVMO spectral range exhibits

pronounced peaks and can be subdivided into the seven components (fig. 1). Despite a certain formalism, this subdivision allows qualitative and quantitative comparisons between the XPS, XES, and $RX_\alpha$-DV calculation results for the $[(UO_2)F_6]^{6-}$ ($D_{6h}$) cluster.

The relativistic calculation results for the ground state of this cluster is given in tab. 1. Since after the electron photoemission the molecule transits into an excited state with a hole on a certain level, the binding energies for the transition states have to be used [12] for a more strict comparison between the theoretical and experimental data. However, in a rough approximation one can suggest that for the valence region the binding energies for the transition state differ from those for the ground state by a constant shift toward the higher absolute energy. Therefore, the present work used the theoretical binding energies increased by 1.2 eV for comparison with the corresponding experimental values (tab. 2). Taking into account the MO compositions (tab. 1) and photoionization cross-sections [13], the theoretical spectral intensities for some energy ranges were determined (tab. 2, fig. 1). Comparing the experimental XPS and theoretical data one has to take into account that the XPS from $UO_2F_2$ reflects the band structure and consists of bands widened due to the solid-state effects. Despite the approximation imperfections, one can see a good qualitative agreement between the theoretical and experimental data. Indeed, the corresponding theoretical and experimental FWHMs ($\Gamma_{theor}$ = 4.5 eV and $\Gamma_{exp}$ = 4.2 eV) and relative intensities of the outer and inner valence bands ($I_{OVMO}^{theor}$ = 42.0%, $I_{IVMO}^{theor}$ = = 58.0% and $I_{OVMO}^{exp}$ = 40.6%, $I_{IVMO}^{exp}$ = = 59.4%) are comparable. A satisfactory agreement between the theoretical and experimental binding energies for some electronic orbitals, in particular the 16 $_7^-$, 9 $_9^-$, and 16 $_7^+$ IVMO, was reached (tab. 2). The worst agreement was reached for the middle (15 $_7^-$-14 $_7^-$) IVMO region. Previously the IVMO XPS structure has been interpreted on the basis of the non-relativistic $X_\alpha$ calculations [4, 5]. It allowed a qualitative identification of the fine spectral structure in the binding energy range 0-23 eV. It was possible because inclusion of relativistic effects in general gives a strong separation of the $U6p_{1/2}$ component, but the main features in the binding energy range 0-23 eV remained invariable. The relativistic calculation allowed a qualitative and quantitative interpretation of the XPS fine structure in the whole range 0-40 eV.

Despite the fact that the outer valence band intensity for uranium compounds is mostly due to the U5f,6d and O(F)2p AOs, for uranium oxides $UO_2$, $UO_3$, and fluorite $UF_4$ it has been shown on the basis of the conversion electron spectra that the inner valence U6p electrons participate effectively in the OVMO formation [14-16]. Using this and the data of tab. 2 in mind one can suggest that the U6p elec-

trons participate in the OVMO formation in $UO_2F_2$. Also, experimental evidence for the fact that the U5f electrons can participate in the chemical bond without loosing their f-nature was practically established. Indeed, the experimental intensity ratio OVMO/IVMO is 0.68, which is comparable with the corresponding theoretical value 0.72 (tab. 2). Since the U5f AO practically does not participate in the IVMO formation, the difference can be explained by the decrease of the photoionization cross-section of the U5f electrons participating in the chemical bond. It contradicts the traditional in chemistry by suggesting the excitation of the U5f electrons to the U6d shell before the chemical bond formation. Therefore, one can suggest that the relativistic calculation results reflect the partial U5f electronic density rather well (tab. 2). These data show that more than two U5f electrons participate in the chemical bond formation, and the vacant U5f states are located within 6 eV near the absorption edge (tab. 1).

In the IVMO XPS range the good agreement was reached only for the 16 $_7^-$, 9 $_9^-$, 16 $_7^+$, and 13 $_7^-$ orbitals characterizing the spectral width. Taking into account the comparability of the theoretical data and experimental total relative intensity, one can suggest that the calculated energies of the 15 $_7^-$-14 $_7^-$ IVMO differ significantly from the corresponding experimental data (tab. 2).

Taking into account the non-relativistic calculations for the $[(UO_2)F_6]^{4-}$($D_{6h}$) cluster [7] and experimental data on the core-valence levels binding energy differences for uranium [17] and $UO_2F_2$ [1-4], in the molecular orbitals as linear combinations of atomic orbitals approximative MO schematic diagram can be built (fig. 2). This diagram enables the understanding of the real XPS structure of $UO_2F_2$. In this approximation one can separate formally the $16\gamma_7^-(3)$, $14\gamma_7^-(6)$, and $13\gamma_7^-(9)$ IVMO group characterizing the interatomic distance U-O in uranyl group $UO_2^{2+}$, $9\gamma_9^-(4)$, $15\gamma_7^-(7)$, and $8\gamma_9^-(8)$ IVMO characterizing the interatomic distance U-L in the equatorial plane, as well as the quasiatomic $16\gamma_7^+(5)$, $5\gamma_8^-(8)$, $8\gamma_9^+(8)$, $5\gamma_8^+(8)$, and $15\gamma_7^+(8)$ IVMOs attributed generally to the O(F)2s-$U6p_{1/2}$ electrons. It has to be noted that this IVMO subdivision is well grounded [1, 6]. The experimental data show that the binding energies of quasiatomic $5\gamma_8^-(8)$-$15\gamma_7^+(8)$ IVMOs have to be close to 29.9 eV, which differs significantly from results of theoretical calculation. Indeed, the F1s and F2s binding energies for $UO_2F_2$ are 685.3 and 29.9 eV respectively and $\Delta E_i$(F1s-F2s) = 655.4 eV [1, 6]. In support of this one can note the similar $\Delta E_i$ values of 655.4 and 655.2 eV for $MnF_2$ and $MnF_3$ respectively [18] where the F2s AOs participate weakly in the MO formation. It allowed a more exact determination of the IVMO sequence order (compare tab. 1 and tab. 2, fig. 2). Since the binding energies of the quasiatomic F2s related orbitals increase by

**Table 2. XPS parameters of the UO$_2$F$_2$ and UO$_2$F$_6^{4-}$ (D$_{6h}$) cluster at $R_{U-O}$ = 1.74 10$^{-10}$ m and $R_{U-O}$ = 2.43 10$^{-10}$ m ($R$ X$_\alpha$-DVM) and the U6p and U5f electronic state densities $\rho_i$(e$^-$)**

| MO | $-E^{(c)}$ [eV] | X-ray photoelectron spectra | | | U6p and U5f electronic state densities $\rho_i$ (e$^-$) | | | |
| | | Energy$^{(d)}$ [eV] | Intensity [%] | | | | | |
| | | Experiment | Theory | Experiment | 5f$_{5/2}$ | 5f$_{7/2}$ | 6p$_{3/2}$ | 6p$_{1/2}$ |
| **OVMO** $21\gamma_7^{+(a)}$ | 4.1 | | 0.3 | | | | | |
| $13\gamma_9^-$ | 4.3 | | 0.7 | | | | | 0.08 |
| $21\gamma_7^-$ | 4.5 | | 0.3 | | | | | |
| $8\gamma_8^+$ | 4.7 | | 0.3 | | | 0.06 | | |
| $8\gamma_8^-$ | 4.9 | | 1.1 | | | 0.10 | | |
| $12\gamma_9^-$ | 4.9 | | 1.6 | | | 0.12 | | |
| $20\gamma_7^-$ | 5.1 | | 2.6 | | | | | 0.16 |
| $7\gamma_8^+$ | 5.1 | | 0.3 | | | | | |
| $12\gamma_9^+$ | 5.1 | | 0.3 | | | | | |
| $20\gamma_7^+$ | 5.1 | | 0.3 | | | | | |
| $11\gamma_9^+$ | 5.3 | | 0.3 | | | | | |
| $11\gamma_9^-$ | 5.5 | | 0.3 | | | 0.14 | | |
| $7\gamma_8^-$ | 5.5 | | 2.1 | | | | | |
| $19\gamma_7^-$ | 5.6 | | 0.6 | | | | 0.02 | |
| $19\gamma_7^+$ | 6.0 | | 0.6 | | 0.02 | | | |
| $6\gamma_8^-$ | 6.2 | | 0.8 | | | | | |
| $6\gamma_8^+$ | 7.0 | | 1.0 | | 0.04 | | | |
| $10\gamma_9^+$ | 7.0 | | 1.0 | | | 0.52 | | |
| $18\gamma_7^-$ | 7.1 | 5.6 (3.1) | 12.0 | 29.3 | | | | 0.34 |
| $18\gamma_7^+$ | 8.2 | | 1.6 | | 0.24 | 0.26 | | |
| $10\gamma_9^-$ | 8.2 | 8.3 (3.2) | 6.2 | 11.3 | | | | 0.12 |
| $9\gamma_9^+$ | 8.5 | | 0.7 | | 0.14 | 0.06 | | |
| $17\gamma_7^-$ | 8.6 | | 6.3 | | | | 0.06 | |
| $17\gamma_7^+$ | 8.6 | | 0.7 | | 0.36 | | | |
| $I_i^{(b)}$ | | | 42.0 | 40.6 | 0.80 | 1.26 | 0.08 | 0.70 |
| **IVMO** $16\gamma_7^-$ | 15.6 | 15.6(3.5) | 7.1 | 7.3 | | | 0.06 | 0.94 |
| $9\gamma_9^-$ | 19.4 | 19.8(3.5) | 8.7 | 10.4 | | | | 1.74 |
| $16\gamma_7^+$ | 22.9 | 23.0(3.5) | 6.5 | 6.3 | | | | |
| $15\gamma_7^-$ | 23.2 | 26.5(2.5) | 4.4 | 4.3 | | | 0.24 | 0.08 |
| $5\gamma_8^-$ | 23.2 | | 3.6 | | | | | |
| $8\gamma_9^+$ | 23.3 | | 3.6 | | | | | |
| $5\gamma_8^+$ | 23.4 | 29.9(3.5) | 3.6 | 14.7 | | | | |
| $15\gamma_7^+$ | 24.0 | | 3.7 | | | | | |
| $8\gamma_9^-$ | 24.0 | | 4.0 | | | | | 0.14 |
| $14\gamma_7^-$ | 30.6 | 25.0(3.5) | 6.6 | 10.4 | | | 0.52 | 0.48 |
| $13\gamma_7^-$ | 31.7 | 32.1(3.5) | 6.2 | 6.0 | | | 1.12 | 0.08 |
| $I_i^{(b)}$ | 47.6 | 49.3(6.0) | 58.0 | 59.4 | | | 1.94 | 3.46 |
| $14\gamma_7^+$ | | | ~8.0 | | | | | |

$^{(a)}$ Upper filled MO (2 electrons), filling number for all orbitals is 2
$^{(b)}$ Total U6p electronic state densities and peak intensities
$^{(c)}$ Binding energies shifted by 1.2 eV toward the higher values
$^{(d)}$ FWHMs are given in parentheses

about 6 eV, the F2s contribution to, for example, the $9\gamma_9^-(4)$ IVMO must decrease, and to the $13\gamma_7^-(9)$ IVMO must increase. The contribution of the U6p$_{3/2}$ AO to the $8\gamma_9^-(8)$ IVMO must decrease, which agrees with the experimental data. In this case the separation of the $8\gamma_9^-(8)$ IVMO from the general band of quasiatomic orbitals (8) is not possible (tab. 2). Taking into account that $\Delta E_U$ = 360.6 eV, $\Delta E_1$ = 363.6 eV, one can find $\Delta_2$ = 3.0 eV and $\Delta_1$ = 4.2 eV [1, 6]. The perturbation is $\Delta_3$ = 2.6 eV. The peak width of the quasiatomic orbitals $16\gamma_7^+(5)$ and $5\gamma_8^-(8)$- (8) is comparable to the widths of other IVMOs. The observed narrowing of the $15\gamma_7^-(7)$ IVMO can be explained by the partial loss of the antibonding nature due to the mixture of the (7%) of O2s AO (tab. 2, see also [11]).

For comparative quantitative analysis of the experimental and theoretical intensities the considered spectra were decomposed having in mind data in fig. 2. The diagram of fig. 2 was built on the basis of the experimental binding energies and theoretical intensities. The identification of the XPS structure is shown in tab. 2 and fig. 2. These data show that the experimental and theoretical binding energies practically coincide. However, the experimental IVMO intensities often differ significantly from the corresponding theoretical values. The best agreement was reached for the $16\gamma_7^-(3)$, $16\gamma_7^+(5)$, and $13\gamma_7^-(9)$ IVMOs. The theoretical data show that 0.78 U6p e$^-$ electrons participate in the OVMO formation (tab. 2), where the U6p$_{3/2}$ electrons take the main part. The U6p distribution in OVMO and IVMO reflects the distribution of the U6p partial electronic density in the valence band of UO$_2$F$_2$. Table 2 also shows that more than two U5f electrons partici-
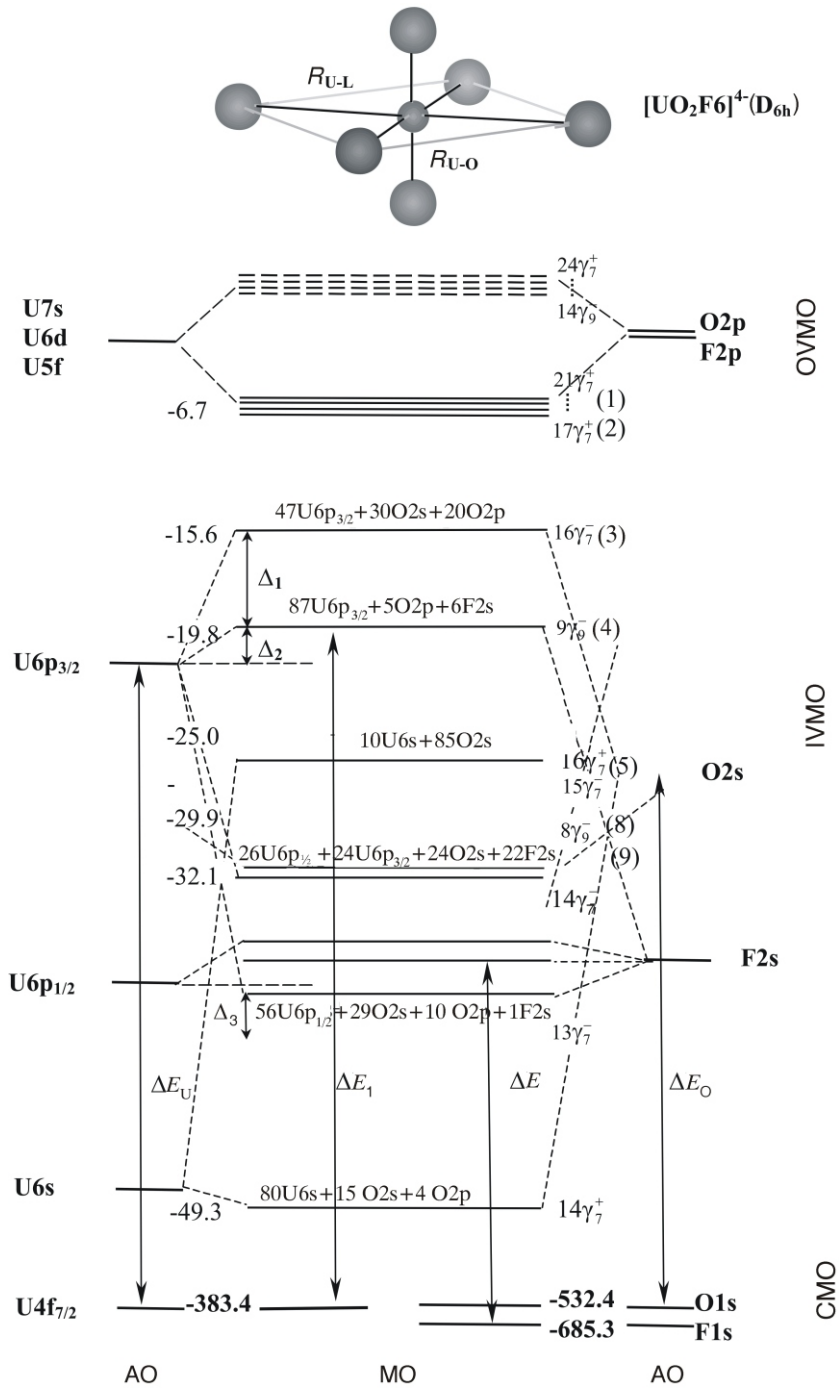
**Figure 2. MO schematic diagram for the $[(UO_2)F_6]^{4-}(D_{6h})$ cluster built on the basis of the theoretical and experimental data. Chemical shift is not shown. Arrows indicate some experimentally measurable binding energy differences. Experimental binding energies in eV are given to the right. Energy scale is not kept.**

pate in the OVMO formation, while in the IVMO formation these electrons do not participate.

Since quantum mechanics can predict qualitatively the alterations of considered spectral intensities depending on the binding energy, one can vary the initial data for the initial clusters for a better agreement between the theoretical and experimental data. As it has been shown [6, 11], the wider an MO is, the more of its electrons participate (bonding, antibonding) in the chemical bond. The narrowes peaks are those attributed to antibonding and quasiatomic orbitals. Therefore, the fact that the $15\gamma_7^-$ (7) IVMO line is relatively narrow can be explained by an admixture of the $U6p_{3/2}$

and O2s AOs. Despite the fact that it is difficult to establish reliably the $15\gamma_7^-(7)$ and $13\gamma_7^-(9)$ IVMO line widths, the obtained data allows the conclusion that the antibonding nature of the $15\gamma_7^-(7)$ IVMO is lower than the bonding nature of the $13\gamma_7^-(9)$ IVMO. In other words, electrons from this IVMO couple must bring a positive contribution to the covalent component of the chemical bond in $UO_2F_2$.

The most ambiguous for interpretation is the $15\gamma_7^-(7)$-$8\gamma_9^-(8)$ IVMO XPS region. Comparison of the XPS data for $UO_2F_2$ and $UF_4$ [6] shows that the quasiatomic F2s AO related peak has to be located at 29.9 eV. Apparently, the calculation was not able to give

**Figure 3.** X-ray $O_{4,5}(U)$ emission spectra from $UO_2F_2$ measured at 3 kV (mA) reflecting the U5d U6p,np,5f electronic transitions. Peak numbers correspond to the transition numbers on the diagram (tab. 3, fig. 4).
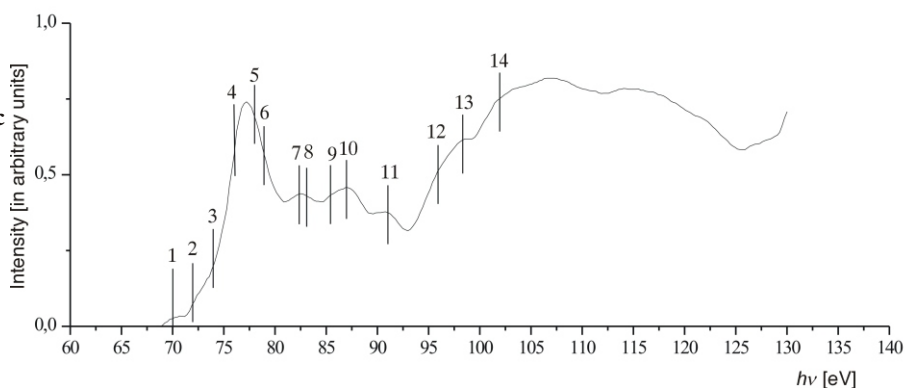
the correct binding energies for these MOs. With this in mind this work carried out the decomposition of this spectral region. The knowledge of the correct IVMO sequence is critical for the understanding of the IVMO contributions to the covalent component of the chemical bond in $UO_2F_2$. The observed peaks (10) in the spectra can be partially attributed to the shake up process during the photoemission.

One of the experimental confirmations for the IVMO formation in $UO_2F_2$ is the high resolution X-ray $O_{4,5}(U)$ emission spectral structure. This spectrum reflecting the $U5d_{5/2,3/2}$ U6p$_{3/2,1/2}$,np,5f $[(O_{4,5}(U)$  $P_{2,3},O_6(U)]$ electronic transitions was observed in the photon energy range $60 < h\nu < 130$ eV and in the higher energy part interfered with the absorption spectrum, which distorted its structure (fig. 3). During the interpretation of the low resolution X-ray $O_{4,5}(U)$ emission spectral structure [19] it has been suggested that the low energy structure is associated with the ternary electronic transitions involving the core uranium shells $U5d_{5/2,3/2}$ U6p$_{3/2,1/2}$. However, fig. 3 shows that ignoring the participation of the U6p$_{3/2,1/2}$ electrons in the IVMO formation one can not identify the X-ray $O_{4,5}(U)$ emission fine spectral

structure. Therefore, the fact that the U6p shell is not core and participates effectively (experimentally observed) in the IVMO formation was taken into account for a correct interpretation of this structure [11].

The low energy band in the $O_{4,5}(U)$ XES from $UO_2F_2$ is wide and poorly resolved despite a relatively high device resolution (fig. 3). As well as for thorium and uranium oxides [20] it can be partially explained by an extra electronic transitions not indicated in the diagram (fig. 4) reflecting the U6p$_{1/2}$,6s-O(F)2p,2s related IVMOs.

The considered $O_{4,5}(U)$ XES from $UO_2F_2$ in the photon energy range 65-110 eV exhibits 14 (not 6 as expected for atomic U) explicit peaks that can be identified using the XPS data and the U6p and O(F)2s related OVMO and IVMO concept (tab. 3). The peaks reflecting the transitions from the OVMO and 16 $_7^-$ and 9 $_9^-$ IVMO can be most reliably (practically unambiguously) identified since these peaks are narrow in both XPS and XES. These peaks are: $5d_{5/2}$  16 $_7^-$(9), $5d_{3/2}$  16 $_7^-$(11), $5d_{5/2}$  9 $_9^-$(6), $5d_{3/2}$  9 $_9^-$(10), $5d_{5/2}$  OVMO(12), and $5d_{3/2}$  OVMO(14) (tab. 3). Identification of the peaks reflecting the transitions from the bonding 14 $_7^-$ and 8 $_9^-$ IVMOs is more com-

**Figure 4.** Schematic diagram of the energy levels for atomic uranium (a) and the $[(UO_2)F_6]^{4-}$ (D$_{6h}$) cluster reflecting uranium close environment in $UO_2F_2$ (b). Numbers (1) through (11) show the transitions from the IVMO to the core levels. The transitions: $5d_{5/2}$  OVMO (12), $5d_{5/2}$  $5f_{7/2}$(13) and $5d_{3/2}$  OVMO(14) are not shown (see tab. 3)
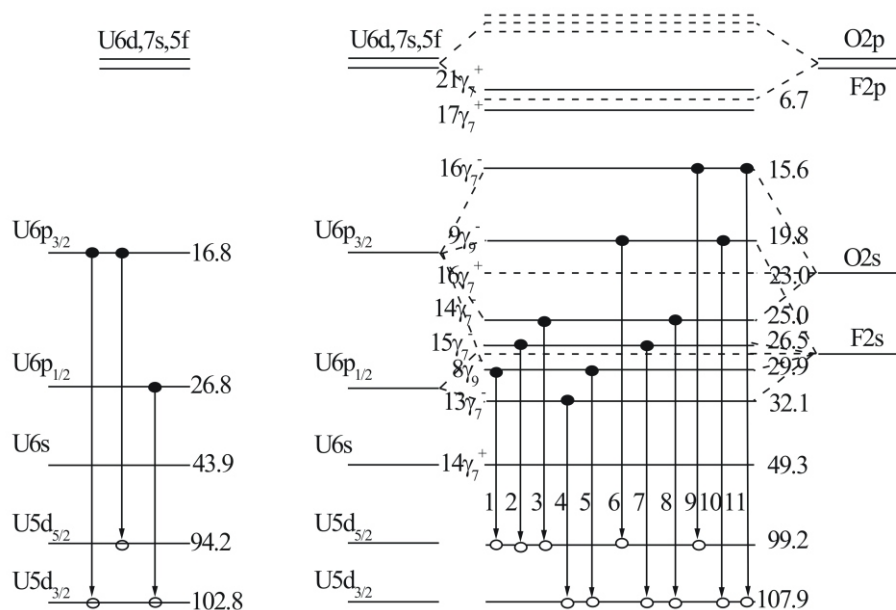
**Table 3. X-ray $O_{4,5}$(U) emission (U5d → U6p,np,5f) transition in U and $UO_2F_2$ on the basis of the XPS and XES data.**

| U | | | $UO_2F_2$ | | |
|---|---|---|---|---|---|
| Transitions | Theory | XPS | Transitions[a] | XPS | XES |
| | | | (1) $5d_{5/2}$ → $8_{9^-}$ | 69.3 | 70.0 |
| | | | (2) $5d_{5/2}$ → $15_{7^-}$ | 72.7 | 72.0 |
| $5d_{3/2}$ → $6p_{1/2}$ | 78.02 | 76.0 | (3) $5d_{5/2}$ → $14_{7^-}$ | 74.2 | 74.0 |
| | | | (4) $5d_{3/2}$ → $13_{7^-}$ | 75.8 | 76.0 |
| $5d_{3/2}$ → $6p_{3/2}$ | 87.28 | 86.0 | (5) $5d_{3/2}$ → $8_{9^-}$ | 78.0 | 78.0 |
| | | | (6) $5d_{5/2}$ → $9_{9^-}$ | 79.4 | 79.0 |
| | | | (7) $5d_{3/2}$ → $15_{7^-}$ | 81.4 | 82.3 |
| $5d_{5/2}$ → $6p_{3/2}$ | 79.11 | 77.4 | (8) $5d_{3/2}$ → $14_{7^-}$ | 82.9 | 83.0 |
| $5d_{5/2}$ → $5f_{5/2}$ | 97.90 | 95.4 | (9) $5d_{5/2}$ → $16_{7^-}$ | 83.6 | 85.4 |
| | | | (10) $5d_{3/2}$ → $9_{9^-}$ | 88.1 | 87.0 |
| $5d_{5/2}$ → $5f_{7/2}$ | 98.64 | 104.0 | (11) $5d_{3/2}$ → $16_{7^-}$ | 92.3 | 91.0 |
| | | | (12) $5d_{5/2}$ → OVMO | 92.5 | 96.0 |
| | | | (13) $5d_{5/2}$ → $5f_{7/2}$ | | 98.3 |
| $5d_{3/2}$ → $5f_{5/2}$ | 106.07 | 104.0 | (14) $5d_{3/2}$ → OVMO | 101.2 | 102.0 |

[a] X-ray O4,5(U) emission peak maxima numbers are given in parentheses (fig. 3)

plicated since the peaks are not that narrow (fig. 3). Despite this some qualitative conclusions can be made. Thus, even the qualitative consideration shows that the low energy region (65-78 eV) of the $O_{4,5}$(U) XES exhibits the structure, which has to be absent in the case of transitions from only atomic $U6p_{3/2,1/2}$ shells. The peaks in this region can be attributed only to the transitions from the IVMOs of the valence band bottom. Thus, the fine $O_{4,5}$(U) XES structure is due to the outer and inner valence molecular orbitals built mostly from the U6p and O(F)2s atomic shells.

We would like to note that despite the approximation imperfections, the calculation results for the $[(UO_2)F_6]^{4-}$ ($D_{6h}$) cluster reflecting uranium close environment in $UO_2F_2$ are in good qualitative agreement with the experimental data, which allowed for the first time a reliable interpretation of the peaks of at least the IVMO ceiling and bottom. These results also can be used for determination of the structure and interatomic distances in uranyl compounds as well as for the interpretation of other X-ray spectra (Auger-, conversion electron, emission, absorption) of uranium compounds.

## CONCLUSIONS

Low binding energy X-ray photoelectron and X-ray $O_{4,5}$(U) emission spectra from $UO_2F_2$ were measured and interpreted in the relativistic $X_\alpha$ Discrete Variation approximation for the $[(UO_2)F_6]^{4-}$ ($D_{6h}$) cluster reflecting uranium close environment in $UO_2F_2$. It yielded a satisfactory qualitative and in some cases quantitative agreement between the theoretical and experimental data.

Despite the traditional opinion that before the chemical bond formation the An5f electrons get promoted to, for example, the An6d atomic orbitals, the theoretical calculations show and experimental data confirm that the An5f atomic shells (more than U5f electrons) can participate directly in the chemical bond formation in uranyl fluorite. The filled U5f states are localized in the OVMO binding energy range from –4 to –9 eV, and the vacant U5f electronic states are generally localized in the low positive energy range (0–6 eV).

The U6p-electrons (about 1 U6p-electron) were experimentally shown to participate significantly in the filled OVMO formation beside the IVMO formation.

The relativistic calculations confirm the fact that the IVMO system associated mostly with the U6p and O(F)2s AOs of uranium and ligands can be subdivided into the two MO groups, one of which ($16_{7^-}$, $14_{7^-}$, $13_{7^-}$) characterizes the bond in the axial direction, and the other one ($9_{9^-}$, $8_{9^-}$) in the equatorial plane. It is important in connection with the development of the experimental technique of determination of the interatomic distances U-L in the axial direction and the equatorial planes of uranyl compounds on the basis of the IVMO XPS parameters.

## REFERENCES

[1] Teterin, Yu. A., Teterin, A. Yu., The Structure of X-Ray Photoelectron Spectra of Light Actinides, *Russian Chemical Reviews, 73* (2004), 6, pp. 588-631

[2] Teterin, Yu. A., Ryzhkov, M. V., Teterin, A. Yu., Panov, A. D., Nikitin, A. S, Ivanov, K. E., Utkin, I. O., The Nature of Chemical Bond in Trioxide -UO$_3$, *Nuclear Technology & Radiation Protection, 17* (2002), 1-2, p. 3-12

[3] Teterin, Yu. A., Teterin, A. Yu., Yakovlev, N. G., Utkin, I. O., Ivanov, K. E., Vukchevich, L., Bek-Uzarov, G. N., X-Ray Photoelectron Study of Actinide (Th, U, Pu, Am) Nitrates, *Nuclear Technology & Radiation Protection, 18* (2003), 2, pp. 31-35

[4] Teterin, Yu. A., Terechov, V. A., Ryzhkov, M. V., Utkin, I. O., Ivanov, K. E., Teterin, A. Yu., Nikitin, A. S., The Role of the U6p,5f Electrons in Chemical Bonding of Uranium Fluorides: X-Ray Photoelectron and X-Ray Emission Studies, *J. Electron Spectrosc. Relat. Phenom., 114-116* (2001), pp. 915-923

[5] Teterin, Yu. A., Terechov, V. A., Ryzhkov, M. V., Utkin, I. O., Ivanov, K. E., Nikitin, A. S., Haritonova, E. D., The Structure of X-ray Photoelectron and O$_{4,5}$(U) Emission Spectra of Uranyl Fluorite Due to the Outer Valence Band Electrons (in Russian), *Poverhnost (Surface), 3* (2001), pp. 44-48

[6] Teterin, Yu. A., Baev, A. S., X-Ray Photoelectron Spectroscopy of Actinide Compounds (in Russian), TsNIIAtominform, Moscow, 1986, p. 102

[7] Teterin, Yu. A., Terechov, V. A., Ryzhkov, M. V., Utkin, I. O., Ivanov, K. E., Teterin, A. Yu., Nikitin, A. S., Haritonova, E. D., Electron Structure of Uranyl Fluoride UO$_2$F$_2$ and the Structure of the X-Ray Photoelectron and O$_{4,5}$(U)-Emission Spectra of the Valence Electrons, *Kondensirovannye Sredy I Mezhfaznye Granitsy, 2* (2000), 1, pp. 83-91

[8] Shirley, D. A., High-Resolution X-Ray Photoemission Spectrum of the Valence Band of *Gold. Phys. Rev. B., 5* (1972), 12, pp. 4709-4714

[9] Mihailov, Yu. N., Chemistry of Platinum and Heavy Elements (in Russian), Nauka, Moscow, 1975, p. 127

[10] Ryzhkov, M. V., Gubanov, V. A., Teterin, Yu. A., Baev, A. S., Electronic Structure and X-Ray Photoelectron Spectra of Uranyl Compounds (in Russian), *Radiohimiya, 1* (1991), pp. 22-28

[11] Teterin, Yu. A., Gagarin, S. G., Inner Valence Molecular Orbitals of Compounds and the Structure of X-Ray Photoelectron Spectra, *Russian Chemical Reviews, 65* (1996), 10, pp. 825-847

[12] Slater, J. C., Johnson, K. H., Self-Consistent-Field X$_\alpha$ Cluster Method for Polyatomic Molecules and Solids, *Phys. Rev. B., 5* (1972), 3, pp. 844-853

[13] Scofield, J. H. Hartree-Slater Subshell Photoionization Cross-Sections at 1254 and 1487 eV, *Journal of Electron Spectroscopy and Related Phenomena, 8* (1976), pp. 129-137

[14] Teterin, Yu. A., Ryzhkov, M. V., Teterin, A. Yu., Panov, A. D., Nikitin, A. S., Ivanov, K. E., Utkin, I. O., XPS Determination of the U6p,5f Electronic States Density in -UO$_3$ (in Russian), *Radiohimiya, 44* (2002), 3, pp. 206-214

[15] Panov, A. D., Zhudov, V. I., Teterin, Yu. A., Conversion Spectra of Electrons of Valence Shells of Oxygen-Containing Uranium Compounds (in Russian), *J. Structural Chem., 39* (1998), 6, pp. 1047-1051

[16] Teterin, Yu. A., The Structure of X-Ray Photoelectron, Emission and Conversion Spectra and Molecular Orbitals in Uranium Compounds (in Russian), *J. Structural Chem., 39* (1998), 6, pp. 1037-1046

[17] Fugle, J. S., Burr, A. F., Watsson, L. M., Fabian, D. Y., Laang, W., X-Ray Photoelectron Studies of Thorium and Uranium, *J. Phys. F: Metal. Phys., 5* (1977), 2, pp. 335-342

[18] Teterin, Yu. A., Teterin, A. Yu., The Structure of X-Ray Photoelectron Spectra of Lanthanide Compounds, *Russian Chemical Reviews, 71* (2002), 5, pp. 403-441

[19] Lyahovskaya, I. I., Ipatov, V. M., Zimkina, T. M., Long-Wave X-Ray 5d Spectra of Thorium and Uranium in Compounds with Oxygen and Fluorine (in Russian), *J. Structural Chem., 18* (1977), 4, pp. 668-672

[20] Teterin, Yu. A., Terechov, V. A., Teterin, A. Yu., Ivanov, K. E., Utkin, I. O., Lebedev, A. M., Vukchevich, L., Inner Valence Molecular Orbitals and Structyre of X-Ray O$_{4,5}$ (Th, U) Emission Spectra in Thorium and Uranium Oxides, *J. Electron Spectrosc. Relat. Phenom., 96* (1998), pp. 229-236

**Игор О. УТКИН, Јуриј А. ТЕТЕРИН, Владимир А. ТЕРЕХОВ, Михаил В. РИЖКОВ, Антон Ј. ТЕТЕРИН, Лабуд ВУКЧЕВИЋ**

## ПРОУЧАВАЊЕ ЕЛЕКТРОНСКЕ СТРУКТУРЕ УРАНИЈУМФЛУОРИТА UO$_2$F$_2$ РЕНДГЕНСКОМ ФОТОЕЛЕКТРОНСКОМ СПЕКТРОСКОПИЈОМ

У раду се разматра фина структура рендгенског фотоелектронског спектра слабо везаних електрона (0-40 eV) и структура рендгенског O$_{4,5}$(U) емисионог спектра из UO$_2$F$_2$. Коришћен је релативистички X$_\alpha$ дискретни варијациони поступак за прорачун [(UO$_2$)F$_6$]$^{4-}$ (D$_{6h}$) кластера који одражава непосредну околину уранијума у UO$_2$F$_2$. Показано је да U5f електрони непосредно учествују у образовању хемијске везе. Такође је показано да U6p електрони учествују у образовању не само унутрашњих, већ и спољашњих валентних молекулских орбитала. Утврђен је секвенцијални поредак унутрашњих валентних молекулских орбитала у подручју енергија везе од 12-40 eV. Ово је од значаја за развој поступка одређивања међуатомских растојања уранијумских једињења у аксијалном правцу и екваторијалној равни, заснованог на рендгенској фотоелектронској спектроскопији.